Check for updates

Received: 23 November 2024 | Revised: 1 April 2025 | Accepted: 15 April 2025

DOI: 10.1111/geoj.70022

THE GJ Royal Geographical Society with IBG

WILEY

ARTICLE

Forecasting urban shifts post-earthquake: LULC change analysis in Elazığ, Turkey using ANN and Markov models

Fatih Sunbul[1] | **Enes Karadeniz**[2] | **Mustafa Taner Sengun**[3] | **Muhammed Kocaoglu**[3]

[1]Faculty of Humanities and Social Sciences, Izmir Bakircay University, Izmir, Turkey

[2]Department of Geography, Faculty of Arts and Science, Inonu University, Malatya, Turkey

[3]Faculty of Humanities and Social Sciences, Fırat University, Elazığ, Turkey

Correspondence
Fatih Sunbul, Faculty of Humanities and Social Sciences, Izmir Bakircay University, Izmir 35665, Turkey.
Email: fatih.sunbul@bakircay.edu.tr

Abstract

Understanding land use and land cover (LULC) dynamics in seismically active regions is crucial for risk-informed urban planning and sustainable post-disaster recovery. This study investigates the impact of the Mw 6.8 Elazığ earthquake (24 January 2020) on LULC patterns in eastern Turkey by integrating high-resolution Sentinel-2 satellite imagery with geographic information systems (GIS), remote sensing (RS), artificial neural networks (ANNs), and Markov chain modelling. The methodology comprises four phases: establishing a pre-earthquake baseline (2015–2019), assessing post-earthquake changes (2015–2023), analysing transition probabilities to identify key LULC drivers, and forecasting land-use scenarios for 2030 and 2050 under seismic and non-seismic conditions. Results reveal that seismic activity significantly accelerates urban expansion, shifting development towards geologically stable zones. By 2050, artificial surfaces are projected to occupy 54.70% of the region under seismic influence, compared to 48.87% without it. Agricultural land is more preserved in the seismic scenario (26.54%) than in the non-seismic case (22.68%), while pasture and meadow areas decline sharply to 6.18%, raising concerns for biodiversity and ecosystem services. These findings emphasise the importance of integrating ecological considerations and seismic risk into land-use planning frameworks. By combining multicriteria decision-making with machine learning-based forecasting, the study offers a replicable and scalable model for balancing urban growth, environmental conservation, and resilience. Framed within interdisciplinary insights from disaster resilience theory, urban governance, and spatial risk modelling, this research contributes to the global discourse on sustainable urban transformation in the face of increasing natural hazards.

KEYWORDS

artificial neural networks, earthquake impact, land use and land cover change, Markov models, urban planning

The information, practices and views in this article are those of the author(s) and do not necessarily reflect the opinion of the Royal Geographical Society (with IBG).

This is an open access article under the terms of the Creative Commons Attribution License, which permits use, distribution and reproduction in any medium, provided the original work is properly cited.

© 2025 The Author(s). *The Geographical Journal* published by John Wiley & Sons Ltd on behalf of Royal Geographical Society (with the Institute of British Geographers).

1 | INTRODUCTION

It is essential to understand land use and land cover (LULC) changes for effective urban planning and disaster risk management, particularly in seismically active regions such as Turkey (Aydöner & Maktav, 2009; Choudhary & Pathak, 2016). LULC dynamics are influenced by both natural processes, such as seismic activity (Ishihara & Tadono, 2017) and anthropogenic drivers like population growth and urban expansion (Kamran et al., 2023; Khan et al., 2014; Sterling & Ducharne, 2008). These changes impact not only the immediate post-disaster landscape but also long-term spatial organisation in both urban and rural environments (Sunbul, 2019). In Turkey, where seismic hazards are persistent and widespread (Kalafat et al., 2021), understanding LULC transformations is critical due to their broad socio-economic and ecological consequences (Desalegn et al., 2014).

This study engages with interdisciplinary concepts that require conceptual clarity due to their variability in the literature. 'Resilience' here refers to the capacity of urban and ecological systems to absorb seismic shocks while reorganising to maintain core functions (Allan et al., 2013; Inzulza Contardo & Moran Figueroa, 2021; Wu & Wu, 2012). 'Sustainability' is approached through economic (e.g., protection of productive land), environmental (e.g., habitat preservation), and social (e.g., housing for displaced communities) lenses (Giddings et al., 2002; Goodland, 2002). While 'land use' focuses on the functional deployment of space (e.g., agriculture, infrastructure), 'land cover' describes the physical characteristics of the Earth's surface (e.g., vegetation, buildings, water bodies) (Aplin, 2004; Friedl et al., 2022; Rindfuss et al., 2008). Although frequently conflated in remote sensing products, this study maintains a conceptual and analytical distinction between the two.

Addressing these multifaceted dynamics requires an interdisciplinary framework that integrates geography, ecology, urban planning, and disaster risk governance (Ghalehteimouri et al., 2024; Wang et al., 2022). Turkey, positioned at the convergence of the African, Arabian, and Eurasian tectonic plates, is among the most seismically active countries in the Mediterranean (Bozkurt, 2001). Major fault systems, including the North Anatolian Fault Zone (NAFZ), East Anatolian Fault Zone (EAFZ), and the Western Anatolian Seismic Zone, define the nation's seismic vulnerability (Dirik & Göncüoğlu, 2010; Duman & Emre, 2013; Şengör et al., 2005). These faults have produced Turkey's most destructive earthquakes, such as the Mw 7.4 Kocaeli event in 1999 (Saatcioglu et al., 2001) and the Mw 6.8 Elazığ event in 2020 (Caglar et al., 2023). Beyond immediate devastation, such events catalyse profound and lasting LULC transformations as regions enter cycles of recovery and reconstruction (Karadeniz & Sunbul, 2023).

The 2020 Elazığ earthquake serves as a critical case for examining how seismic activity accelerates urban encroachment into agricultural and forested lands, posing risks to ecological balance and food security. This case highlights the urgency of integrating sustainable planning principles into post-disaster reconstruction. National frameworks in Turkey have increasingly embraced this orientation. The AFAD Disaster and Emergency Management Strategic Plan (2019–2023) emphasised risk-sensitive spatial planning, while the most recent Strategic Plan (2024–2028) prioritises geospatial modelling, safe relocation zones, and integrated land governance (AFAD, 2025). The alignment with sustainable urban development strategies suggests that ecological concerns, such as biodiversity and ecosystem services, must be integral to future city growth patterns (Takano et al., 2023).

Geospatial technologies, particularly geographic information systems (GIS) and remote sensing (RS), are indispensable in mapping and analysing LULC changes before and after seismic events (Thomas et al., 2007). GIS facilitates spatial decision-making, while RS provides high-resolution imagery to detect subtle landscape transformations (Aydöner & Maktav, 2009; Muttitanon & Tripathi, 2005). When integrated with predictive models like artificial neural networks (ANNs) and Markov chains, these technologies allow for scenario-based projections of post-seismic urban growth and land degradation (Karadeniz & Sunbul, 2023). Our study applies this integration to the Elazığ case, demonstrating how neural network-driven modelling can forecast land transitions and support resilient urban planning (Sharifi & Yamagata, 2018). Among machine learning tools used in LULC forecasting—such as decision trees, support vector machines, or random forests—ANNs combined with Markov chains have shown superior capacity to model non-linear spatial and temporal dynamics (Al-sharif & Pradhan, 2014). Accordingly, this study employs a multi-layer perceptron (MLP) with a transition sub-model, specifically tailored to capture abrupt, post-seismic land-use shifts.

The aim of this research is to analyse LULC changes in Elazığ after the 2020 earthquake and offer a scalable framework for spatial planning in other seismically vulnerable regions. The study follows a four-phase methodology: (1) pre-earthquake LULC analysis (2015–2019); (2) comparative assessment of post-seismic changes (2015–2023); (3) identification of transition drivers such as seismic intensity and urban pressure; and (4) predictive modelling of future land scenarios for 2030 and 2050. By integrating resilience theory, disaster risk perspectives, and spatial modelling, the

14754959, 0, Downloaded from https://rgs-ibg.onlinelibrary.wiley.com/doi/10.1111/geoj.70022 by Turkey Cochrane Evidence Aid, Wiley Online Library on [19/05/2025]. See the Terms and Conditions (https://onlinelibrary.wiley.com/terms-and-conditions) on Wiley Online Library for rules of use; OA articles are governed by the applicable Creative Commons License

proposed framework deepens the understanding of Elazığ's transformation and provides a transferable tool for sustainable, risk-informed urban planning in other earthquake-prone regions.

2 | RESEARCH AREA

Elazığ, located in eastern Turkey within the geologically active Alpine-Himalayan Mountain Range, is positioned at the intersection of the Eurasian, African-Arabian, and Anatolian Plates, making it highly susceptible to seismic activity (Figure 1) (Reilinger et al., 2006). Spanning 38°30′ to 40°0′21″ E longitude and 38°0′17″ to 39°0′11″ N latitude, the province is bordered by Bingöl, Tunceli, Malatya, and Diyarbakır, with the Keban and Karakaya Dam lakes shaping its landscape. The region's geology, reflecting the Tethys Ocean's evolution, includes prominent geological units like the Pontides, Anatolides, and Taurides (Dewey & Şengör, 1979; Ketin, 1966). Historically rooted in the ancient city of Harput, founded around 4000 BC Elazığ transitioned into a modern urban centre after being renamed in 1937. Its population, reaching 604,411 in 2023 (Turkish Statistical Institute, 2023), reflects steady urban expansion driven by economic diversification and rising demand for housing and infrastructure. The economy, dominated by industry, agriculture, and trade, has shifted focus towards mining and industry following the Keban Dam's impact on arable land, with over 1200 industrial operations in the organised industrial zone (Harmanşa & Abut, 2017). Elazığ's location on the East Anatolian Fault Zone (EAFZ), with a 430 km length and 10 mm/year slip rate, places it in a high-risk seismic area, as reaffirmed by earthquake hazard maps and the updated 2018 assessment using peak ground acceleration (PGA) values (Cetin et al., 2021). The devastating 6.8 magnitude Sivrice earthquake on January 24, 2020, with a PGA of 0.292 g, caused widespread destruction, particularly in older buildings, underscoring the urgent need for resilient urban planning and sustainable land use strategies (Sayın et al., 2021).

3 | STUDY DESIGN AND DATA INTEGRATION

This research endeavours to shed light on the potential evolution of land use and land cover (LULC) over a 30-year span in Elazig city, exploring future development trajectories using predictive models. Our approach encompasses systematic computation and modelling, as illustrated in Figure 2. We employ maps detailing location, population, geology, and seismic activity as independent variables in our analysis. These maps serve to visually corroborate the analytical results. Our methodology is informed by the approaches outlined in the seminal work of Rahnama and Wyatt (2021), aligning with established research practices in the field. This alignment demonstrates our commitment to building upon foundational insights provided by previous studies, ensuring our research is both relevant and methodologically sound.

This study adopts a comprehensive framework to analyse and forecast LULC changes in Elazığ, Turkey, focusing on the 2020 earthquake's impacts. Although the analysis covers 2015–2023, this temporal scope effectively captures the rapid post-disaster interventions typical in Turkey. These interventions, led by the Mass Housing Administration (TOKİ), prioritise relocating affected populations to stable areas within short time frames. Following seismic events, geophysical and geological surveys guide the construction of large-scale housing projects, including residential buildings, infrastructure, and amenities, which are typically completed within 2 years. These developments often transform forested and agricultural lands into residential zones and roads, underscoring the swift and substantial impacts of earthquakes on LULC. These new developments were predominantly established in previously non-residential areas such as agricultural and open grassland zones, indicating a clear shift in land allocation priorities. This pattern of urban expansion highlights a departure from pre-earthquake spatial trends, with residential areas spreading into geologically stable but formerly undeveloped peripheries. The research methodology is systematically structured as detailed in the following sub-sections.

3.1 | LULC change analysis (2015–2019)

This initial phase conducts a detailed analysis of LULC dynamics in Elazığ prior to the seismic event. By utilising remote sensing (RS) and geographic information systems (GIS), this stage establishes a baseline understanding of pre-earthquake LULC conditions, which is crucial for meaningful post-event comparisons and further analysis.

14754959, 0, Downloaded from https://rgs-ibg.onlinelibrary.wiley.com/doi/10.1111/geoj.70022 by Turkey Cochrane Evidence Aid, Wiley Online Library on [19/05/2025]. See the Terms and Conditions (https://onlinelibrary.wiley.com/terms-and-conditions) on Wiley Online Library for rules of use; OA articles are governed by the applicable Creative Commons License

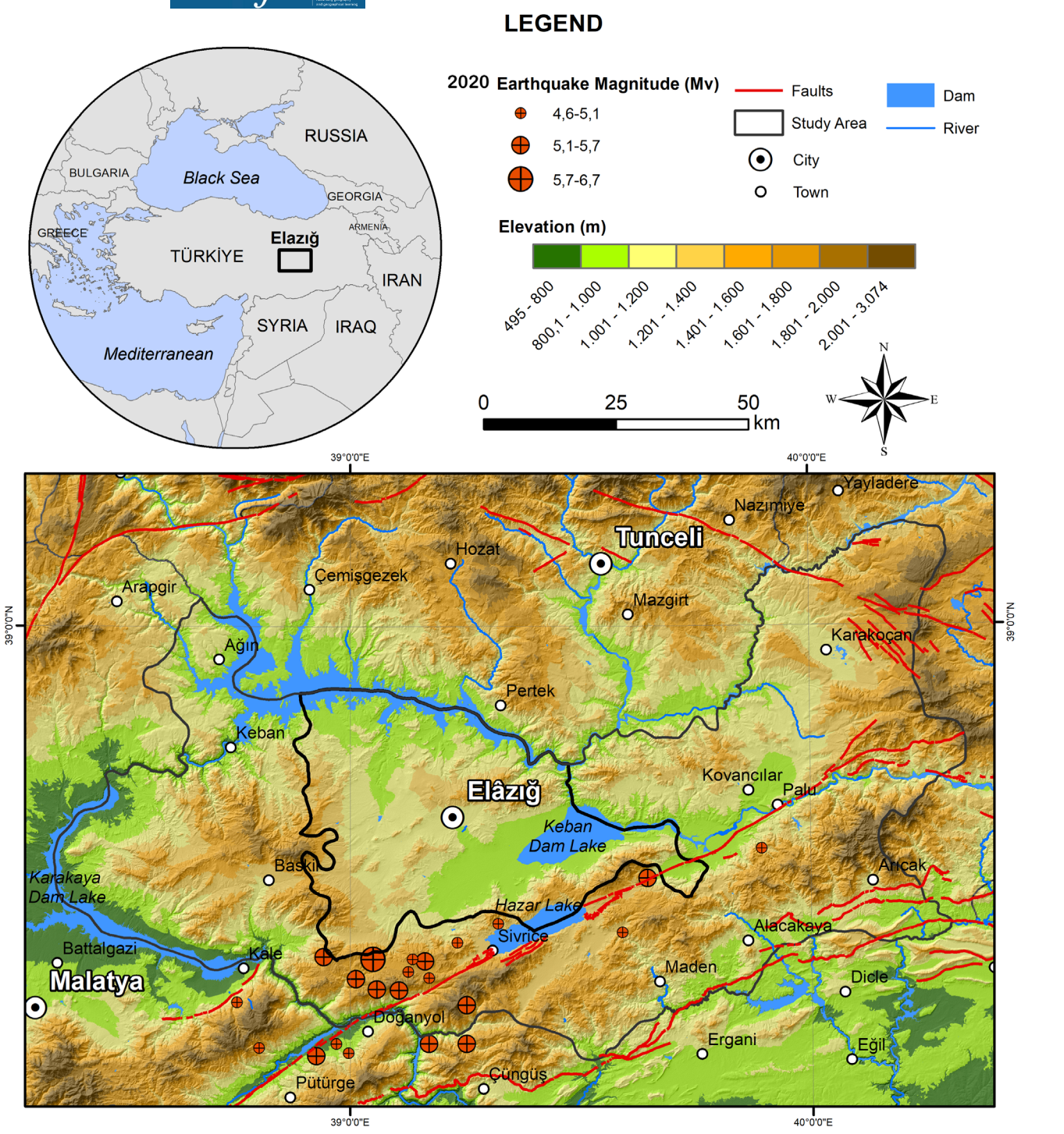

FIGURE 1 Location map of the study area in Elazığ Province, Eastern Turkey. The main map displays key physical features including topography (elevation in meters), lakes and dams (e.g., Keban Dam), stream networks, and active fault lines. Provincial and district boundaries are indicated, along with the Elazığ city centre and adjacent provinces (e.g., Malatya, Bingöl, Diyarbakır). The distribution of seismic events related to the Mw 6.8 Elazığ earthquake on 24 January 2020 is shown, with green circles representing the main shock and aftershocks, categorised by magnitude (4.6–6.7 Mw).

3.2 | Post-seismic LULC assessment (2015–2023)

In the second phase, we evaluate post-earthquake LULC patterns up to 2023. Through a comparative analysis of pre- and post-event LULC data, this stage identifies the direct and indirect impacts of the seismic event on land use and cover, revealing critical changes in land use dynamics induced by the earthquake.

14754959, 0, Downloaded from https://rgs-ibg.onlinelibrary.wiley.com/doi/10.1111/geoj.70022 by Turkey Cochrane Evidence Aid, Wiley Online Library on [19/05/2025]. See the Terms and Conditions (https://onlinelibrary.wiley.com/terms-and-conditions) on Wiley Online Library for rules of use; OA articles are governed by the applicable Creative Commons License

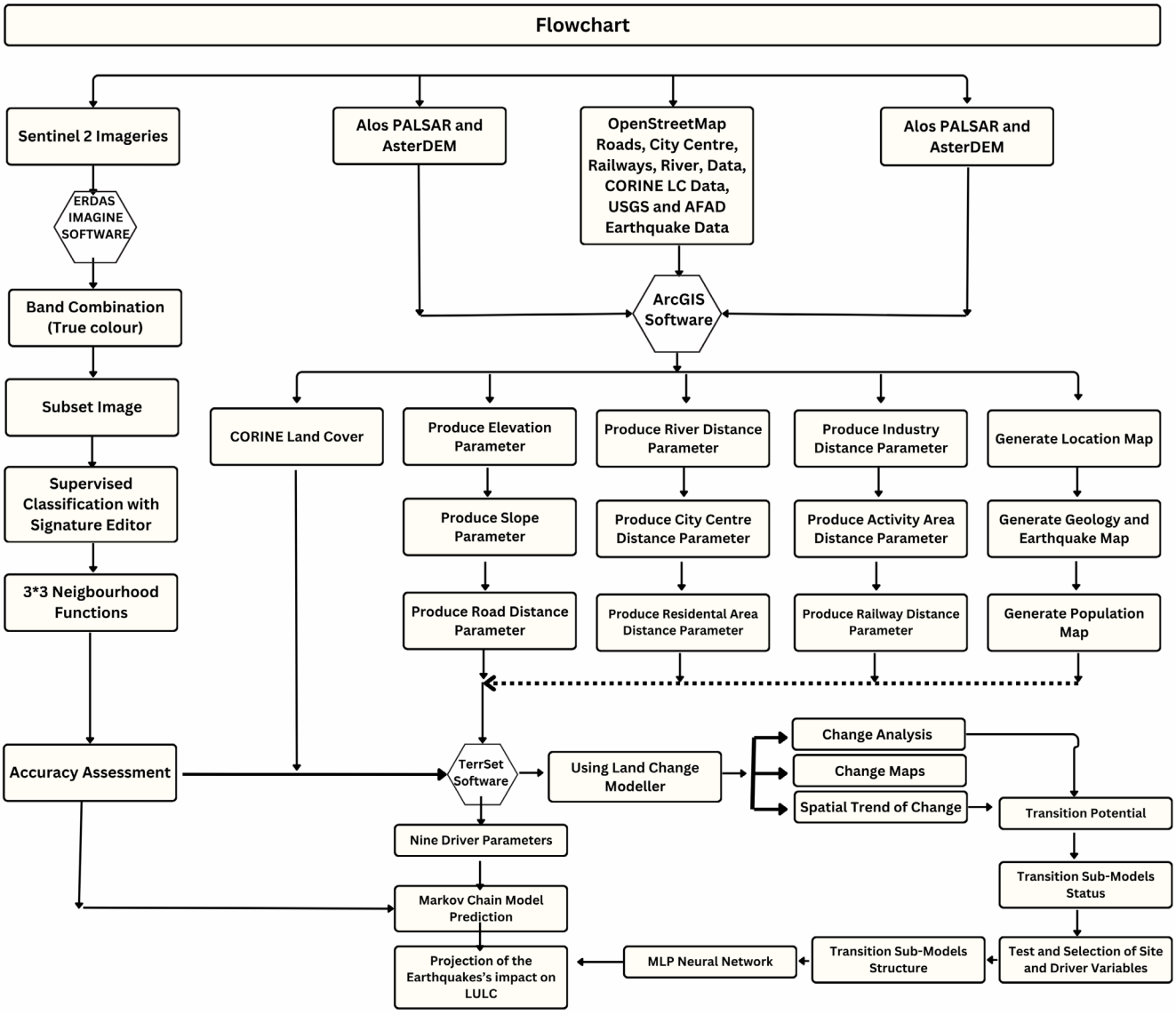

FIGURE 2 Schematic overview of the study framework.

3.3 | Transition probability determination

By analysing multiple influencing factors, such as seismic damage, urban expansion, and agricultural transitions, this phase calculates the transition probabilities within the LULC assessment framework. This analytical process is essential for understanding the underlying mechanisms that drive LULC changes in response to seismic disturbances.

3.4 | Future LULC scenario forecasting

The final phase projects future LULC scenarios for Elazığ in 2030 and 2050. By leveraging the transition probabilities identified in the previous stage, this predictive analysis employs advanced modelling techniques to simulate potential land use configurations under varying environmental and developmental scenarios. The outcomes of this phase will inform strategic urban planning and disaster management efforts aimed at enhancing resilience in earthquake-prone regions. The model outputs further suggest that post-earthquake development patterns diverge significantly from pre-disaster trajectories, indicating a trend towards decentralisation. Rather than intensifying urban cores, new residential growth appears to be oriented towards peripheral and structurally safer regions, which may have long-term implications for transportation, service distribution, and urban connectivity.

14754959, 0, Downloaded from https://rgs-ibg.onlinelibrary.wiley.com/doi/10.1111/geoj.70022 by Turkey Cochrane Evidence Aid, Wiley Online Library on [19/05/2025]. See the Terms and Conditions (https://onlinelibrary.wiley.com/terms-and-conditions) on Wiley Online Library for rules of use; OA articles are governed by the applicable Creative Commons License

This study utilised a diverse array of high-resolution datasets to analyse the 2020 Sivrice/Elazığ earthquake's impact on LULC changes in the region. Key datasets included Sentinel-2 imagery for settlement and landscape changes, digital elevation models (DEMs) for terrain analysis, and OpenStreetMap and Google Earth Pro for infrastructure mapping. Seismic data from the US Geological Survey (USGS) and fault line information from MTA provided insights into earthquake risks, while geopolitical and hydrological context was drawn from Natural Earth and OpenStreetMap. Detailed attributes of these datasets are summarised in Table 1.

For accuracy assessment, satellite images were analysed using a pixel-based supervised classification method in Erdas software, categorising land use into five classes: water bodies, residential zones, agricultural lands, forest and shrubs, and barren areas. A 3×3 neighbourhood analysis was applied to address pixel contamination, refining thematic images. The classification's accuracy was validated with 200 sample points (40 per category) using the equalised random method. Metrics, including producer accuracy (PA), user accuracy (UA), overall accuracy (OA), and the Kappa coefficient (Kc), were calculated via the ERDAS accuracy assessment tool.

$$\mathrm{OA} = \frac{\sum_{i=1}^{r} D_{ii}}{N} \tag{1}$$

$$\mathrm{UA} = \frac{\sum D_{ij}}{x_{+i}} \tag{2}$$

$$\mathrm{PA} = \frac{\sum D_{ij}}{x_{i+}} \tag{3}$$

$$\mathrm{Kappa} = \frac{N \sum_{i=1}^{r} x_{ii-} \sum_{i=1}^{r} \left(x_{i+} * x_{+i}\right)}{N^2 - \sum_{i=1}^{r} \left(x_{i+} * x_{+i}\right)} \tag{4}$$

TABLE 1 Datasets used in the study: sources, acquisition dates, and spatial resolutions.

Dataset	Source	Dates	Spatial resolution (m)
Sentinel images TM, OLI	US Geological Survey (https://earthexplorer.usgs.gov/)	27 August 2015; 21 August 2019; 9 August 2023	10
Digital elevation model (Slope, stream network)	Earthdata ASTER Global Digital Elevation Model V003 (https://search.earthdata.nasa.gov/) Alaska Satellite Facility (https://search.asf.alaska.edu/)	30 November 2013; 9 July 2007	30, 12.5
Roads	OpenStreetMap (https://www.openstreetmap.org/)	2020 1999–2020	Vector, field scale
Earthquakes	US Geological Survey Earthquake Catalogue (https://earthquake.usgs.gov/earthquakes/)	1957–2021	Vector, field scale
Active faults	Gen. Directorate of Mineral Research and Exploration GeoScience MapViewer and Drawing Editor (http://yerbilimleri.mta.gov.tr/)	2013	1:1.250,000
Countries and maritime borders, Water surface	Natural Earth (https://www.naturalearthdata.com/) OpenStreetMap (https://www.openstreetmap.org/)	2018 2020	1:10,000,000 Vector; Vector, field scale

Note: Data retrieved from U.S. Geological Survey (Earth Explorer), NASA Earthdata (ASTER GDEM), Alaska Satellite Facility (ASF Data Search), OpenStreetMap, Google Earth Pro, USGS Earthquake Catalogue, MTA GeoScience, and Natural Earth, accessed in July 2024.

14754959, 0, Downloaded from https://rgs-ibg.onlinelibrary.wiley.com/doi/10.1111/geoj.70022 by Turkey Cochrane Evidence Aid, Wiley Online Library on [19/05/2025]. See the Terms and Conditions (https://onlinelibrary.wiley.com/terms-and-conditions) on Wiley Online Library for rules of use; OA articles are governed by the applicable Creative Commons License

In this context, r represents the number of rows in the error matrix, while x_{ii} refers to the number of observations found at the intersection of row i and column i (on the main diagonal). The term x_{+i} represents the total number of observations in row i, and x_{i+} signifies the total number of observations in column i. N denotes the total number of observations in the entire matrix. A Kappa value exceeding 0.80 is considered to indicate almost perfect agreement (Wang et al., 2022). The classification accuracy for the LULC categories approached 90%, with the Kappa coefficient (κ) consistently exceeding 0.87 (Table 2).

Predictive modelling plays a vital role in analysing LULC changes, with models like ANNs, cellular automata (CA), and Markov chains widely used for their predictive accuracy and integration capabilities (Noszczyk, 2019; Verburg et al., 2004). Among these, the MLP-Markov model effectively combines GIS and RS data, addressing the Markov model's limitation of spatial characteristics through ANN integration (Rahnama & Wyatt, 2021).

The MLP-Markov chain integration, chosen for its effectiveness in merging spatial pattern recognition with temporal dynamics, has distinct advantages over alternative methods such as CA-Markov and logistic regression-Markov models. Specifically, its capability to incorporate diverse and high-resolution spatial datasets provides enhanced accuracy in predicting post-disaster urban development, as demonstrated in previous seismic studies (Pahlavani et al., 2017; Wang et al., 2022). While CA-Markov models offer spatial simulation based on cellular principles, they may oversimplify complex spatial relationships, especially in irregular post-seismic transformations. Logistic regression-Markov, on the other hand, can suffer from lower spatial resolution and a limited ability to capture nonlinear dependencies. In contrast, the MLP-based approach allows for the integration of multi-source data and the modelling of intricate spatial–temporal patterns, making it particularly suitable for environments undergoing rapid LULC shifts following seismic disruptions.

ANNs, inspired by human neural networks, are valued for their ability to process diverse data and establish relationships between LULC and driving factors (Dang & Kawasaki, 2016; Noszczyk, 2019). Markov chains, using transition probability matrices, predict temporal changes but benefit from MLP's spatial capabilities, offering a robust approach for LULC forecasting by integrating spatial and temporal dynamics (Pahlavani et al., 2017):

$$S_{(t,t+1)} = P_{ij} \times S_{(t)} \tag{5}$$

Here, $S(t)$ represents the condition of the system at the selected time t, and $S_{(t+1)}$ indicates the condition at the subsequent time, $t+1$. P_{ij}, the state transition matrix, is illustrated in the subsequent matrix P

$$P = P_{ij} = \begin{bmatrix} p_{11} & \cdots & p_{1m} \\ \vdots & \ddots & \vdots \\ p_{m1} & \cdots & p_{mm} \end{bmatrix}, \left(0 \le P_{ij} \le 1\right) \tag{6}$$

The transition matrix, P_{ij}, and the Markov probability matrix facilitate the prediction of land use changes, showcasing the probability of transitions between states (Krumbein & Dacey, 1969). By integrating MLP with the Markov chain model, we leverage the strengths of both approaches: the spatial pattern recognition capabilities of ANNs and the temporal predictive power of Markov chains. This combined model allows for more accurate and comprehensive LULC

TABLE 2 Evaluation of the LULC classification accuracy throughout the study.

	2015		2019		2023	
Land use/land cover classes	**Producer accuracy (%)**	**User accuracy (%)**	**Producer accuracy (%)**	**User accuracy (%)**	**Producer accuracy (%)**	**User accuracy (%)**
Residential area	94.00	95.45	92.00	98.57	95.71	95.00
Agriculture	96.00	96.00	98.00	89.78	90.32	87.78
Pasture	91.67	100.0	94.74	100.00	90.00	100.00
Park and orchard	100.00	76.00	98.47	97.56	98.00	88.89
Barren area	92.59	100.0	84.21	88.89	82.50	91.67
Overall accuracy (%)	92.59		92.00		90.00	
Kappa coefficient (κ)	0.90		0.89		0.87	

14754959, 0, Downloaded from https://rgs-ibg.onlinelibrary.wiley.com/doi/10.1111/geoj.70022 by Turkey Cochrane Evidence Aid, Wiley Online Library on [19/05/2025]. See the Terms and Conditions (https://onlinelibrary.wiley.com/terms-and-conditions) on Wiley Online Library for rules of use; OA articles are governed by the applicable Creative Commons License

predictions, accommodating both spatial dependencies and temporal dynamics. In this study, the ANN-Markov model was customised by fine-tuning the training iterations and hidden layer architecture to accommodate high-resolution Sentinel-2 imagery and spatial transition characteristics specific to Elazığ. Transition sub-model parameters were adjusted based on proximity variables (e.g., distance from roads, city centre, and rivers), reflecting local post-disaster urbanisation dynamics. These modifications enabled the model to better capture non-linear spatial dependencies induced by seismic disruption.

4 | DATA ANALYSIS

4.1 | Driving variables

Land use and land cover (LULC) changes result from the interplay of anthropogenic, abiotic, and biophysical factors, shaped by socio-economic, political, and environmental forces (Weng, 2001). For the Elazığ plain, nine critical parameters were identified, categorised as dynamic or static. Dynamic variables, such as proximity to urban areas, roads, railways, industrial zones, rivers, and attractions, reflect human activity and infrastructure development. Static variables, including elevation and slope, provide consistent topographical context, influencing land-use decisions over time (Figure 3).

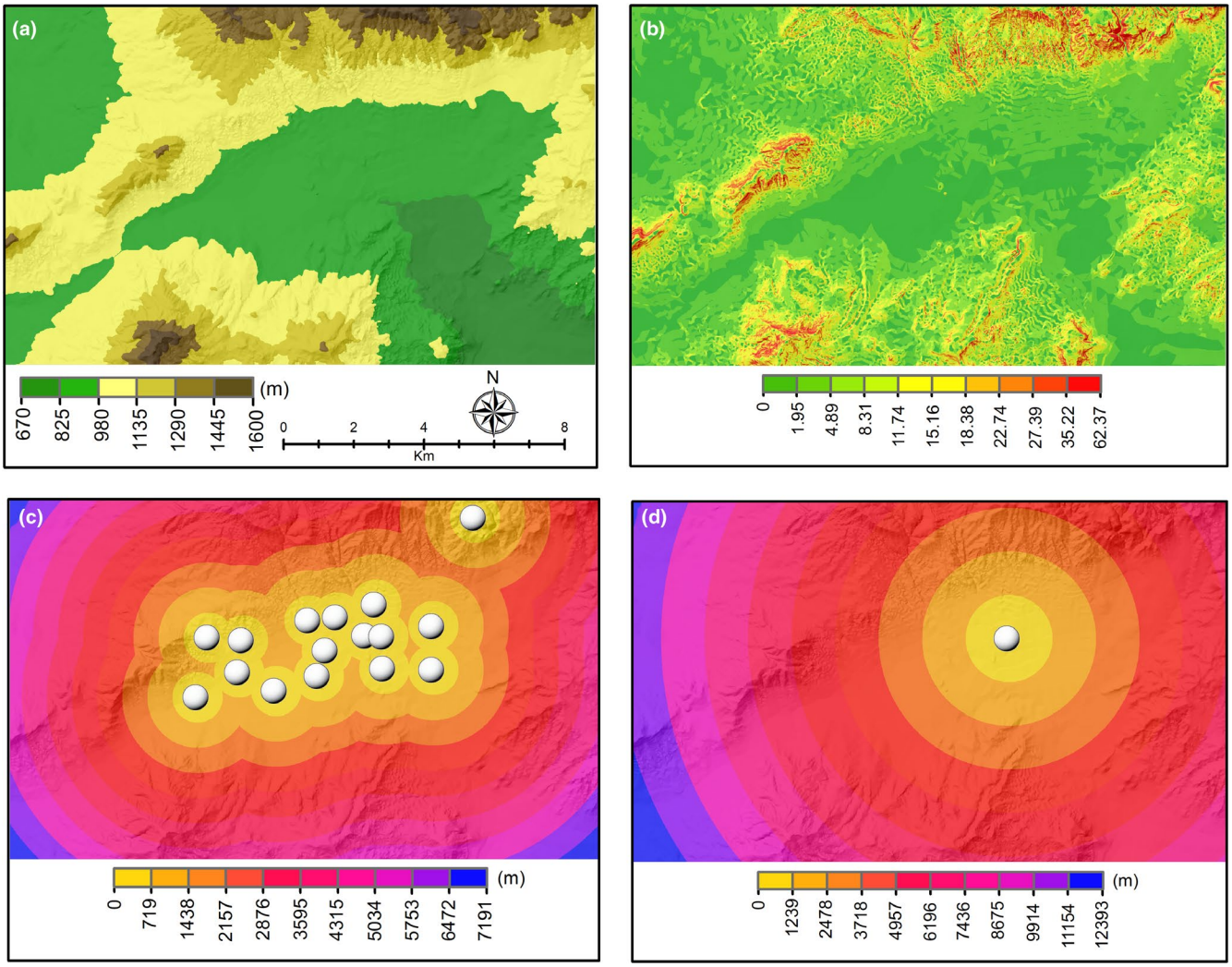

FIGURE 3 Map of driving variables: (a) Elevation, (b) Slope, (c) Industry distance, (d) Distance from activity area, (e) Distance from city centre, (f) Distance from residential area, (g) Distance from roads, (h) Distance from railways, (i) Distance from river.

14754959, 0, Downloaded from https://rgs-ibg.onlinelibrary.wiley.com/doi/10.1111/geoj.70022 by Turkey Cochrane Evidence Aid, Wiley Online Library on [19/05/2025]. See the Terms and Conditions (https://onlinelibrary.wiley.com/terms-and-conditions) on Wiley Online Library for rules of use; OA articles are governed by the applicable Creative Commons License

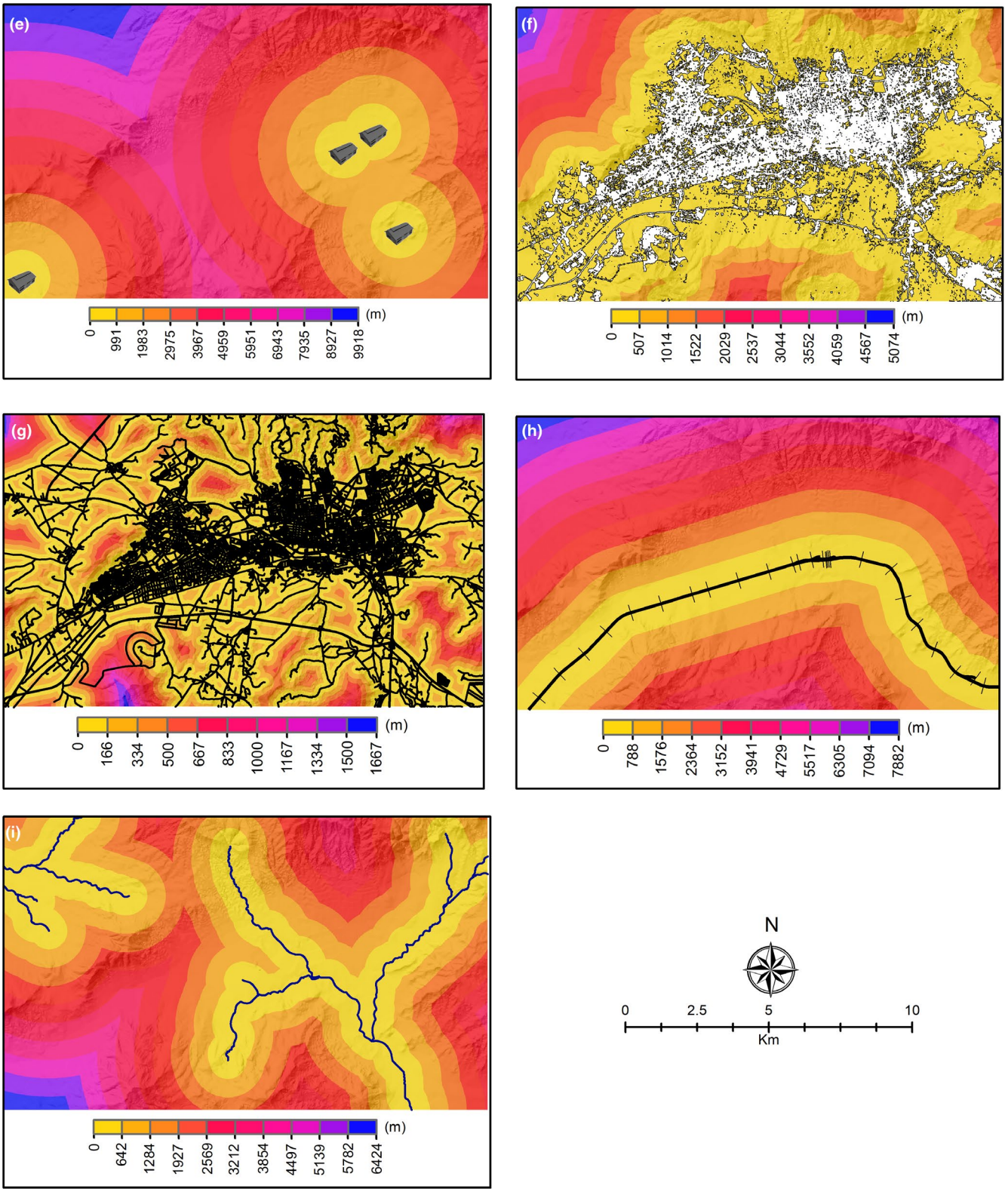

FIGURE 3 (Continued)

Significant land-use transitions were observed in residential, agricultural, pasture, and bare areas, with urban expansion leading to a noticeable shift from agricultural and forest land to residential development. Similarly, increased demand for agricultural production caused shifts from forest to agricultural areas. In order to model these changes, we used the TerrSet software and its transition sub-model function to create two primary sub-models:

14754959, 0, Downloaded from https://rgs-ibg.onlinelibrary.wiley.com/doi/10.1111/geoj.70022 by Turkey Cochrane Evidence Aid, Wiley Online Library on [19/05/2025]. See the Terms and Conditions (https://onlinelibrary.wiley.com/terms-and-conditions) on Wiley Online Library for rules of use; OA articles are governed by the applicable Creative Commons License

TABLE 3 Cramer's value of driver variables across the study region.

Land use class	Distance from urban	Distance from roads	Distance from city centre	Distance from streams	Distance from railways	Distance from industry	Distance from activity areas	Dem	Slope
Overall value	0.2628	0.2514	0.2481	0.1573	0.2021	0.1896	0.2477	0.2209	0.1825
Artificial (Residential) area	0.4212	0.4438	0.3640	0.1107	0.3115	0.2270	0.4456	0.2256	0.1965
Agriculture	0.3482	0.2438	0.3407	0.1752	0.2490	0.2750	0.3025	0.1485	0.0946
Pasture and meadow	0.2264	0.2383	0.1605	0.1826	0.1825	0.1591	0.1706	0.3096	0.2470
Park andorchard	0.0782	0.0755	0.1400	0.1577	0.1148	0.1295	0.1016	0.1901	0.0848
Barren area	0.1858	0.1682	0.2266	0.1472	0.1396	0.1700	0.1417	0.1733	0.2153

Sub-model (a): Captures the transition from agricultural and forest areas to residential zones, driven by urban expansion and infrastructure development.
Sub-model (b): Focuses on the shift from forest areas to agricultural land, driven by economic pressures for agricultural production.

Following sub-model creation, additional steps such as site selection and river variable assignment were carried out using TerrSet commands. To assess the relationship between driving variables and observed LULC changes, Cramer's *V* statistic was calculated for each variable. Cramer's *V* provides a measure of the strength of association between these categorical variables and land-use transitions, offering insights into the most influential factors in the study area. The slope variable showed the weakest relationship (Cramer's $V = 0.1534$), while proximity to the city centre had the strongest influence on land-use changes (Cramer's $V = 0.2537$). As recommended by Cohen (1988), variables with Cramer's *V* values above 0.15 were included in the analysis to ensure statistical significance. The Cramer's *V* values, detailed in Table 3, reveal the varying influence of each variable on different land-use types, providing a deeper understanding of the driving forces behind LULC changes in the Elazığ plain.

4.2 | Land use transition

The Mw 6.8 earthquake in Elazığ on 24 January 2020 caused widespread damage to infrastructure and significant shifts in settlement patterns, particularly in central districts. A damage assessment conducted by May 2021 evaluated 4352 buildings, finding 1567 collapsed or severely damaged and 884 of 983 moderately damaged buildings further deteriorated after the 27 December 2020 earthquake (Dogan et al., 2021). A comparison of urban development maps from 2019 to 2022 revealed rapid conversion of previously uninhabited state lands into residential zones, reshaping the urban landscape in response to the disaster.

To forecast land use changes, the transition sub-model and MLP-Markov model analysed pre- and post-earthquake scenarios. One scenario modelled urban growth driven by socio-economic factors, while the other incorporated the earthquake's impacts, predicting LULC changes for 2030 and 2050 (Rahnama & Wyatt, 2021). Transition probability matrices generated using the Markov chain algorithm quantified changes over time, offering a robust framework for capturing seismic disruptions (Lambin, 2006; Petit et al., 2001). Sentinel-2 imagery from 2015, 2019, and 2023 highlighted rapid urbanisation and significant shifts in both urban and natural landscapes during recovery, underscoring the earthquake's profound influence on Elazığ's land use dynamics (Figure 4).

4.3 | Observed scenario

The Mw 6.8 earthquake on 24 January 2020 significantly reshaped Elazığ's urban and natural landscapes, causing extensive infrastructural damage and altering settlement patterns. Comparative analysis of LULC data from 2015, 2019, and 2023 reveals substantial shifts in land use categories over time. In 2015, agricultural areas dominated the landscape, covering 5962 hectares (34.42%), followed by pasture and meadows (5395 hectares, 31.15%), and artificial surfaces (3990 hectares, 23.04%). Parks and orchards accounted for 825 hectares (4.76%), while bare land comprised 1147 hectares (6.62%).

14754959, 0, Downloaded from https://rgs-ibg.onlinelibrary.wiley.com/doi/10.1111/geoj.70022 by Turkey Cochrane Evidence Aid, Wiley Online Library on [19/05/2025]. See the Terms and Conditions (https://onlinelibrary.wiley.com/terms-and-conditions) on Wiley Online Library for rules of use; OA articles are governed by the applicable Creative Commons License

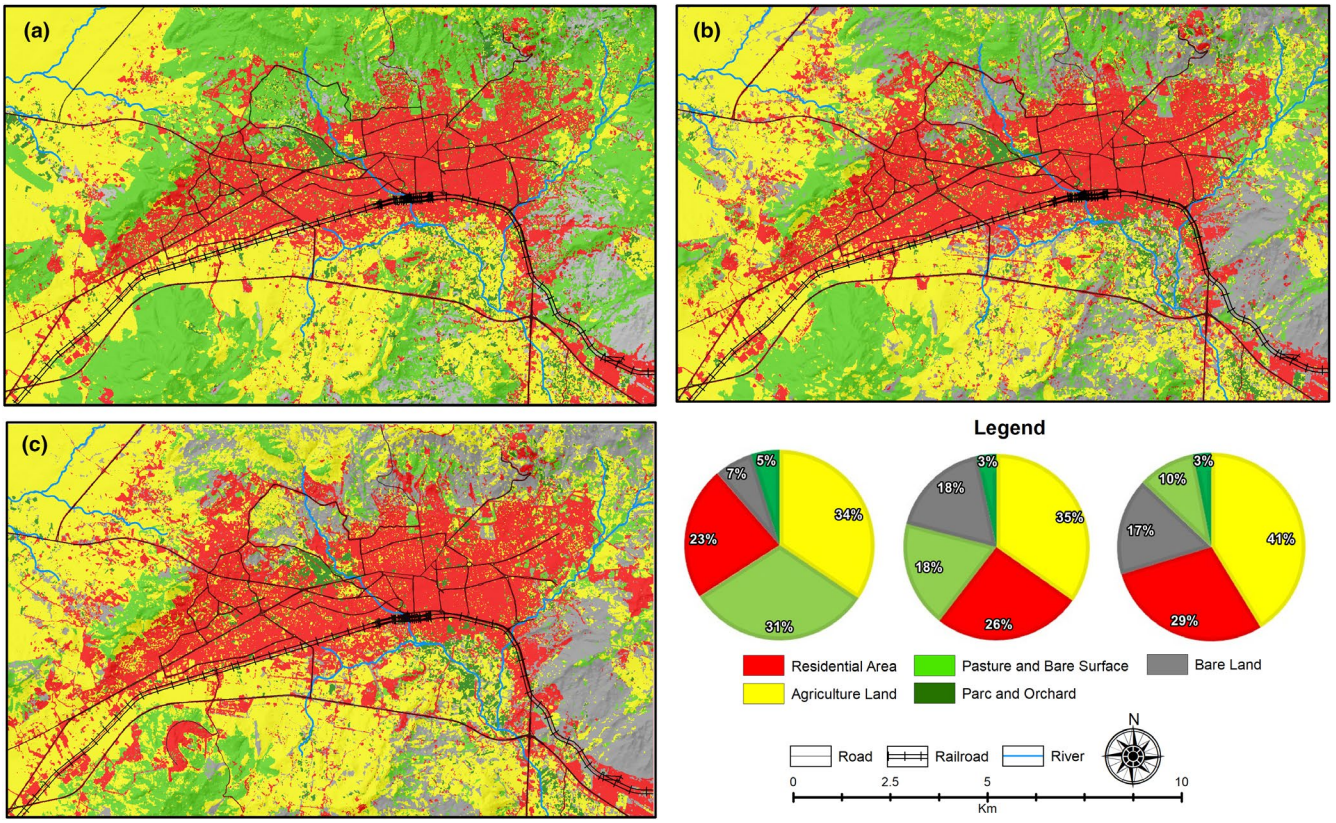

FIGURE 4 Spatiotemporal visualisation of LULC in Elazığ across three time points. Images are ordered clockwise: (a) (2015), (b) (2019), (c) (2023).

By 2019, artificial surfaces expanded to 4646 hectares (26.83%), reflecting urban encroachment driven by population growth and socio-economic pressures. Pasture and meadow areas declined sharply to 3211 hectares (18.54%), while bare land nearly doubled to 2864 hectares (16.54%), indicating land degradation. Parks and orchards reduced to 586 hectares (3.38%), underscoring mounting urban development pressures.

Post-earthquake recovery efforts between 2019 and 2023 accelerated these changes. Artificial surfaces expanded by 616 hectares to 5262 hectares (30.38%), representing a 31.9% increase since 2015, driven by the need to rebuild infrastructure and accommodate displaced populations. Agricultural areas grew substantially to 7147 hectares (41.27%), reflecting strategic efforts to enhance food security and rural resilience.

Although the population in 2023 is reported, the net demographic trajectory remains ambiguous. While initial displacement likely reduced central urban density, reconstruction projects and housing incentives appear to have supported partial return migration. However, no definitive population data is currently available to determine whether the region has experienced net growth or decline. This demographic uncertainty highlights the importance of integrating real-time population monitoring into post-disaster planning and recovery frameworks.

Meanwhile, pasture and meadow lands continued their sharp decline, falling to 1735 hectares (10.02%) – a 67.86% decrease from 2015 – underscoring the significant transformation of natural landscapes. Bare land decreased slightly to 2660 hectares (15.36%) in 2023, potentially indicating early signs of stabilisation or land recovery. Parks and orchards further diminished to 515 hectares (2.97%), reflecting sustained pressure on green spaces. Overall, these land use changes illustrate the profound impact of the earthquake on Elazığ's spatial dynamics and emphasise the challenges of balancing rapid reconstruction with long-term environmental and agricultural sustainability.

The data reveal a rapid urbanisation process, accelerated by post-earthquake reconstruction. The 31.9% increase in artificial surfaces since 2015 reflects not only immediate disaster recovery efforts but also ongoing trends in urban development driven by population growth and economic factors. Agricultural areas expanded by 1185 hectares (19.88%) between 2015 and 2023, likely influenced by the need to bolster food production, shifts in land use policies, and economic incentives. However, the sharp decline of pasture and meadow areas by 3660 hectares (67.86%) over the same period raises concerns about environmental sustainability, as grassland loss impacts biodiversity, soil health, and carbon sequestration. Fluctuations in bare land – rising to 2864 hectares in 2019 and slightly decreasing to 2660 hectares in 2023

14754959, 0, Downloaded from https://rgs-ibg.onlinelibrary.wiley.com/doi/10.1111/geoj.70022 by Turkey Cochrane Evidence Aid, Wiley Online Library on [19/05/2025]. See the Terms and Conditions (https://onlinelibrary.wiley.com/terms-and-conditions) on Wiley Online Library for rules of use; OA articles are governed by the applicable Creative Commons License

– suggest a combination of construction activities, land clearing, and later stabilisation. The loss of 310 hectares of parks and orchards since 2015 underscores the vulnerability of green spaces amid urban expansion, emphasising the need for balanced land management practices.

The dynamic transformation of Elazığ's land use patterns highlights the complexities of post-disaster recovery. Extensive urban and agricultural growth has come at the expense of natural and recreational landscapes, underscoring the importance of integrating sustainable development principles into land use planning. High-resolution Sentinel-2 satellite imagery proved critical for capturing these changes, offering detailed and timely data for urban planners and policymakers. By combining remote sensing data with predictive modelling techniques like the transition sub-model and MLP-Markov model, this study provides a robust framework for evaluating land use dynamics in seismically active regions. These tools enable the assessment of future scenarios, supporting strategies to enhance resilience and sustainable development in the face of natural disasters.

4.4 | Comparison of 2030 LULC projections

The projected LULC for Elazığ in 2030, modelled using MLP neural networks and Markov chain methods, illustrates two distinct trajectories under seismic (with earthquake scenario, WES) and non-seismic (without earthquake scenario, WOES) conditions (Figure 5). In the WOES, urban growth follows traditional patterns, extending into adjacent agricultural plains and along existing infrastructure. By 2030, artificial surfaces are projected to cover 39.58% (6854 hectares), reflecting a 30% increase from 2023, while agricultural areas shrink to 31.74% (5497 hectares). Pasture and meadow lands reduce to 16.76% (2903 hectares), and parks and orchards decline to 3.29% (570 hectares). Bare land decreases to 8.63% (1495 hectares), indicating development pressures on open spaces. This scenario highlights a cost-driven expansion with limited consideration of seismic safety, focusing on economic growth at the expense of agricultural and natural landscapes.

In contrast, the WES incorporates the 2020 earthquake's influence, redirecting urban growth towards geologically stable areas on higher ground, prioritising safety over cost-efficiency. Urban surfaces are projected to expand to 41.01% (7102 hectares), while agricultural areas slightly increase to 34.93% (6049 hectares), reflecting efforts to preserve fertile lands. Pasture and meadow lands decline sharply to 8.69% (1505 hectares), converted to urban and agricultural uses. Parks and orchards grow modestly to 3.76% (652 hectares), suggesting an emphasis on integrating green spaces into safer urban layouts. Bare land rises to 11.61% (2011 hectares), driven by land clearing for reconstruction and unusable terrain identification. These scenarios underscore the critical role seismic considerations play in shaping land use planning. While the WOES perpetuates traditional urban sprawl, the WES reflects a strategic shift prioritising safety, resilience, and ecological balance, demonstrating the importance of proactive, risk-informed land use policies to enhance urban sustainability and disaster preparedness.

The comparison highlights a strategic effort under the WES to balance urban growth with agricultural preservation. The increase in agricultural land from 31.74% in the WOES to 34.93% in the WES reflects a deliberate move to redirect development towards geologically stable areas, protecting fertile plains for agricultural use. However, the sharp reduction in pasture and meadow lands, from 16.76% to 8.69%, suggests these zones are more vulnerable to conversion when seismic safety is prioritised. The slight increase in parks and orchards under the WES (from 3.29% to 3.76%) indicates an emphasis on integrating green spaces into safer urban layouts, enhancing resilience and liveability. The rise in bare land, to 11.61% in the WES compared to 8.63% in the WOES, likely stems from land clearing for reconstruction or the abandonment of unsafe areas. This underscores the importance of sustainable land management practices to rehabilitate or repurpose such spaces. Overall, these projections demonstrate the value of integrating seismic risk assessments into land use planning. By focusing on geologically stable zones, Elazığ can mitigate seismic risks, protect vital agricultural resources, and maintain ecological integrity. These insights are essential for policymakers and urban planners aiming to promote resilience and sustainable development in the face of future seismic events.

4.5 | Comparison of 2050 LULC projections

The comparison of 2050 projections under the WOES and WES highlights the significant impact of seismic events on land use and urban development strategies (Figure 5). Under the WOES, artificial surfaces are projected to expand to 48.87% of the area, driven by traditional urban sprawl into agricultural lands. In contrast, the WES anticipates a more substantial expansion to 54.70%, reflecting a strategic focus on geologically stable areas to enhance seismic safety. Agricultural

14754959, 0, Downloaded from https://rgs-ibg.onlinelibrary.wiley.com/doi/10.1111/geoj.70022 by Turkey Cochrane Evidence Aid, Wiley Online Library on [19/05/2025]. See the Terms and Conditions (https://onlinelibrary.wiley.com/terms-and-conditions) on Wiley Online Library for rules of use; OA articles are governed by the applicable Creative Commons License

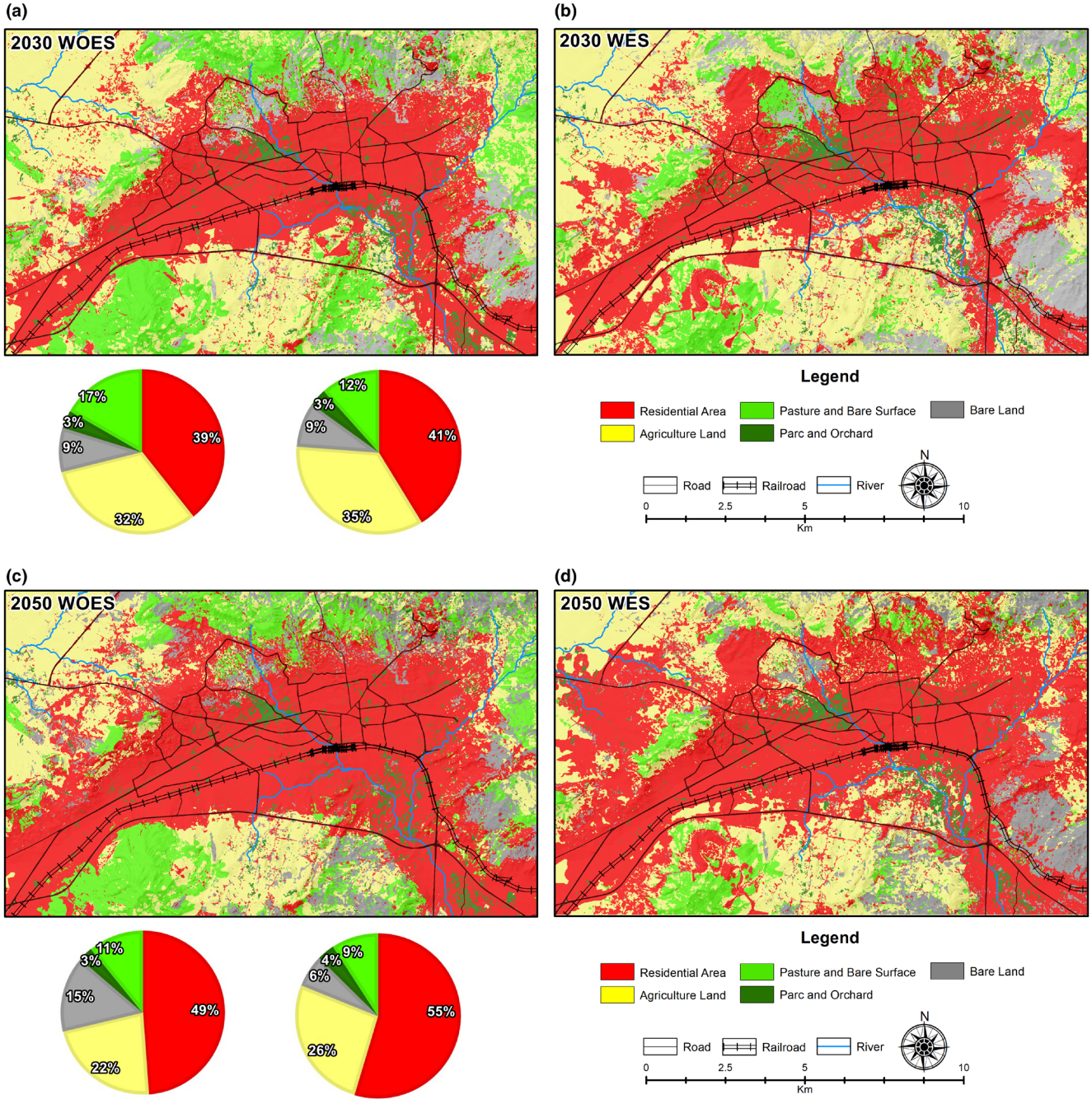

FIGURE 5 Land use projections for 2030 under two scenarios: (a) without earthquake scenario (WOES); (b) with earthquake scenario (WES); Land use projections for 2050 under two scenarios: (c) without earthquake scenario (WOES); (d) with earthquake scenario (WES).

lands see a sharper decline under the WOES, dropping to 22.68%, while the WES preserves more at 26.54%, balancing urban growth with food security. Pasture and meadow lands decline more dramatically in the WES, reducing to 6.18%, compared to 14.60% in the WOES, as these lands are often converted to urban uses due to their geologically stable nature. Parks and orchards slightly increase in the WES to 3.23%, highlighting an effort to integrate green spaces into safer urban layouts, while bare land decreases to 9.35%, reflecting efficient use of previously undeveloped solid ground for urban expansion. Post-2020 earthquake observations illustrate a shift in Elazığ's urban growth patterns, with dispersed expansion replacing concentrated development. Decision-makers prioritised geologically stable sites, transforming former grasslands and bare lands into new urban centres while deprioritising less stable areas. This shift redefined the city's functional dynamics, increasing land values in stable zones and reducing demand in vulnerable southern plains. The emphasis on geological stability represents a paradigm shift in urban planning, prioritising safety and resilience over

14754959, 0, Downloaded from https://rgs-ibg.onlinelibrary.wiley.com/doi/10.1111/geoj.70022 by Turkey Cochrane Evidence Aid, Wiley Online Library on [19/05/2025]. See the Terms and Conditions (https://onlinelibrary.wiley.com/terms-and-conditions) on Wiley Online Library for rules of use; OA articles are governed by the applicable Creative Commons License

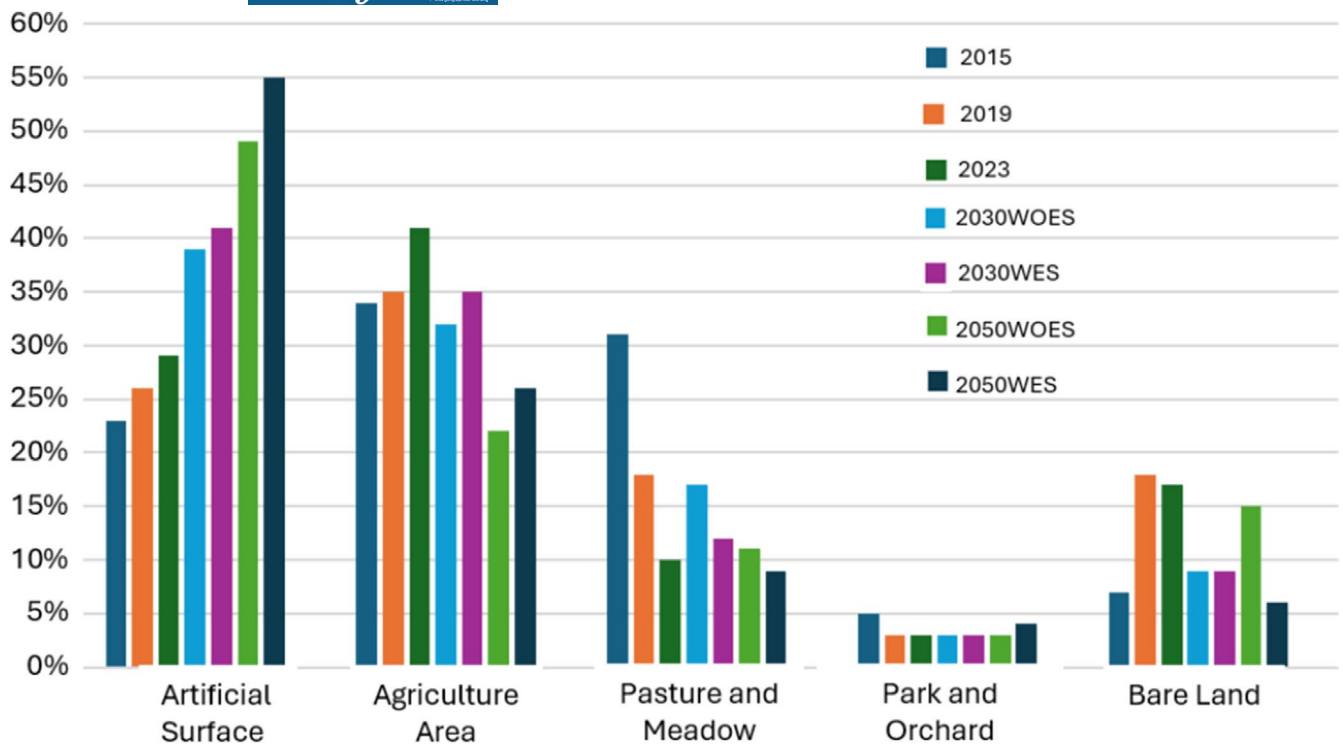

FIGURE 6 Temporal changes in land class distributions over time under different scenarios. (AG, agricultural areas; BL, bare land; PB, pasture and meadow; PO, parks and orchards; RA, residential area; WES, with earthquake scenario; WOES, without earthquake scenario).

traditional economic drivers. By integrating seismic risk assessments, Elazığ's urban planning approach demonstrates how disasters can catalyse sustainable development, balancing urbanisation with the preservation of agricultural and ecological resources to enhance long-term resilience.

Figure 6 illustrates the temporal changes in LULC from historical data to projected scenarios for 2030 and 2050, under both earthquake-impacted (WES) and non-earthquake (WOES) conditions. Residential areas (RA) show a notable increase, particularly under earthquake scenarios. By 2050, residential areas are projected to cover over 55% under the WES compared to 39% in the 2030 WOES. This surge reflects the urgent need for housing and infrastructure reconstruction post-disaster, accelerating urban expansion into geologically stable regions. Conversely, agricultural areas (AG), which peak in 2022, decline in both scenarios but drop below 30% by 2050 under the WES. This sharp decline highlights the significant conversion of agricultural lands into urban uses following seismic events, raising concerns about food security and biodiversity loss.

Pasture and meadow lands (PB) consistently decrease across all timelines, with more pronounced declines under earthquake scenarios, reflecting a shift from natural land covers to urbanised uses. Parks and orchards (PO) remain relatively stable, with slight increases by 2050, underscoring opportunities to incorporate green spaces into urban redevelopment. Bare land (BL) shows modest increases under earthquake scenarios, likely due to land clearing for reconstruction or abandonment of unsuitable areas, while non-earthquake scenarios exhibit more stability, preserving challenging terrains like elevated slopes. These projections emphasise the role of seismic events as catalysts for significant shifts in urban development patterns. The acceleration of urbanisation post-earthquake, coupled with the loss of agricultural and natural lands, underscores the need for integrated planning approaches that prioritise safety, sustainability, and resilience. By balancing reconstruction demands with long-term environmental and social considerations, policymakers can foster sustainable and resilient urban futures for regions like Elazığ.

5 | DISCUSSION AND CONCLUSION

This study analyses lLand use and land cover (LULC) changes in Elazığ, Turkey, following the Mw 6.8 earthquake on 24 January 2020. By integrating high-resolution Sentinel-2 satellite imagery with predictive modelling techniques (specifically the transition sub-model and the multi-layer perceptron (MLP) Markov model), this study analyses observed

14754959, 0, Downloaded from https://rgs-ibg.onlinelibrary.wiley.com/doi/10.1111/geoj.70022 by Turkey Cochrane Evidence Aid, Wiley Online Library on [19/05/2025]. See the Terms and Conditions (https://onlinelibrary.wiley.com/terms-and-conditions) on Wiley Online Library for rules of use; OA articles are governed by the applicable Creative Commons License

land-use changes (2015–2023) and projects future scenarios for 2030 and 2050 under both seismic (WES) and non-seismic (WOES) conditions. The results show that seismic activity significantly accelerates urbanisation and induces notable shifts in land use patterns. By 2050, artificial surfaces are projected to reach 54.70% under WES, compared to 48.87% under WOES, indicating a strategic spatial redistribution of development towards geologically stable regions and a growing prioritisation of hazard avoidance over traditional land value considerations.

This spatial reorientation reflects a broader paradigm shift in post-disaster urban development, where risk perception increasingly shapes land-use decision-making. Comparable transitions have been observed globally. Tian et al. (2022) reported reductions in cultivated and forested lands and increases in construction zones in China's Longxi River Basin after the Wenchuan earthquake. Similarly, Kang et al. (2022) documented increased fragmentation and ecological degradation in Wenchuan County. In Iran, Badri et al. (2006) showed how post-disaster resettlement led to livelihood loss, particularly when displaced populations were disconnected from agricultural land and social networks. In Haiti, Miller (2020) found that informal post-disaster settlements preserved traditional spatial structures such as the *lakou*, sustaining food production, social capital, and mutual support in the absence of formal aid. These cases highlight that land-use transformation following disasters is not merely a physical process, but also reflects deeper socio-economic trade-offs, cultural adaptations, and resilience mechanisms. The Elazığ findings align with these global patterns, underscoring that such transformations are part of systemic responses to environmental shocks.

By combining predictive spatial modelling with empirical satellite data, the study contributes not only to local reconstruction efforts but also to the broader discourse on resilience-based urban transformation. Its multi-scalar analysis aligns with global frameworks such as the Sendai Framework (UNDRR, 2015) and resonates with the increasing scholarly emphasis on adaptive urban planning under Anthropocene conditions.

The results underscore the uneven impacts of seismic activity on agricultural land, emphasising the need to reconcile post-disaster urban expansion with the preservation of productive landscapes. Under the WOES scenario, agricultural land is projected to decline to 22.68% by 2050 due to unregulated urban encroachment, while the WES scenario preserves 26.54% – a gap with serious implications for food security and socio-economic resilience. International evidence supports these findings: post-Manjil earthquake resettlements in Iran disrupted agricultural livelihoods (Badri et al., 2006), whereas in Haiti, the *lakou* – a decentralised, kin-based settlement system – enabled subsistence farming and social cohesion in the absence of formal recovery frameworks (Miller, 2020). In Turkey, top-down reconstruction policies often disregard local land rights, accelerating rural land loss and cultural erosion (Özdoğan et al., 2024). These patterns affirm the need for integrated land management in early recovery (Chang et al., 2010).

Another critical outcome is the sharp decline in pasture and meadow lands under the WES scenario, dropping to 6.18%, a development with serious implications for biodiversity and ecological stability. Similar landscape transformations were observed in post-tsunami Japan, where rice paddies evolved into abandoned or grassland zones, contributing to long-term ecological degradation (Ishihara & Tadono, 2017). These trends emphasise the need for ecological sensitivity in disaster recovery, supporting approaches like United Nations Environment Programme's ecosystem-based disaster risk reduction (Eco-DRR) (Renaud et al., 2016), which advocates continuous ecological monitoring and restoration in urban reconstruction strategies.

The expansion of artificial surfaces in geologically safer areas under WES reflects a deliberate spatial strategy aligned with multi-criteria decision-making frameworks (Opricovic & Tzeng, 2003), which balance redevelopment needs with hazard avoidance. By incorporating criteria such as spatial risk, accessibility, and land suitability, these frameworks help optimise post-disaster land-use decisions. The Elazığ case illustrates the value of predictive modelling in enabling planners to navigate trade-offs between socio-economic resilience and geophysical vulnerability.

The analytical framework is grounded in disaster resilience theory and risk-informed urban planning. The shift of built-up areas towards geologically stable zones aligns with the 'Build Back Better' paradigm (UNDRR, 2015), which promotes integrating hazard mitigation into reconstruction. The customised application of ANNs with Markov chain modelling provides a novel contribution, especially in earthquake-specific LULC forecasting, an area where such approaches are not yet widely adopted (Mondal et al., 2020; Rani et al., 2023). Configured according to local geospatial variables, this model enhances spatial analysis and offers a transferable tool for seismically active regions.

Further analysis identified proximity to urban cores, roads, and industrial areas as key transition drivers. The highest Cramer's V value (0.2628) was observed for distance to urban centres, indicating a clear preference for reconstruction near existing infrastructure. This aligns with earlier findings on the centrality of connectivity in post-disaster land transformation (Ghorbani Kalkhajeh & Jamali, 2019). Incorporating these variables into spatial planning can help prevent

14754959, 0, Downloaded from https://rgs-ibg.onlinelibrary.wiley.com/doi/10.1111/geoj.70022 by Turkey Cochrane Evidence Aid, Wiley Online Library on [19/05/2025]. See the Terms and Conditions (https://onlinelibrary.wiley.com/terms-and-conditions) on Wiley Online Library for rules of use; OA articles are governed by the applicable Creative Commons License

ad-hoc expansion. Moreover, fuzzy logic-based decision support systems (e.g., Kandel et al., 2014) offer tools to manage qualitative and uncertain data in complex post-disaster scenarios.

The integration of high-resolution Sentinel-2 imagery with ANN-based forecasting and multicriteria evaluation provided a solid foundation for identifying land cover dynamics before and after the earthquake. This combined approach enhances spatial accuracy and supports strategic planning in disaster-prone regions. However, limitations persist, such as satellite misclassification, limited socio-economic data, and lack of real-time validation. To improve model reliability and realism, future research should incorporate participatory mapping, ground-truthing, and longitudinal socio-economic assessments.

While this study centres on the 2020 Elazığ earthquake, the catastrophic coupled earthquakes of February 2023 in south-eastern Turkey, impacting many of the same regions, highlight the ongoing relevance of predictive LULC modelling. These successive events further justify the emphasis on geologically safer zones under the WES scenario. Future applications of this framework should incorporate multi-hazard dynamics and cascading effects, reinforcing the need for adaptable and forward-looking reconstruction strategies. Ultimately, resilient post-disaster planning must balance immediate recovery priorities with long-term ecological and social sustainability.

ACKNOWLEDGEMENTS

The authors would like to express their sincere gratitude to Prof. Peter Hopkins and Dr. Johanna Bullard for their valuable editorial guidance and support throughout the review process. We also extend our appreciation to the anonymous reviewers for their insightful comments and constructive suggestions, which greatly improved the quality and clarity of this manuscript.

DECLARATION OF AI USE

The authors declare that no artificial intelligence (AI) tools were used in the writing, editing, data analysis, or production of this manuscript. All work was conducted manually by the authors.

CONFLICT OF INTEREST STATEMENT

The authors declare no conflicts of interest related to this work.

DATA AVAILABILITY STATEMENT

All data referred to in this study are available from the corresponding author and will be made available upon request by email.

ETHICS STATEMENT

This study did not involve human or animal subjects and needed no institutional approval.

ORCID

Fatih Sunbul https://orcid.org/0000-0002-3590-374X
Enes Karadeniz https://orcid.org/0000-0003-0757-8553
Mustafa Taner Sengun https://orcid.org/0000-0003-4039-6591
Muhammed Kocaoglu https://orcid.org/0000-0003-0956-1210

REFERENCES

AFAD. (2025) *AFAD strategic plans (2019–2023 and 2024–2028)*. Disaster and Emergency Management Authority (AFAD), Ministry of Interior, Republic of Türkiye. Available from: https://www.afad.gov.tr/stratejik-planlar [Accessed 16th February 2025].

Alaska Satellite Facility. (n.d.) *ASF data search*. University of Alaska Fairbanks. Available from: https://search.asf.alaska.edu/ [Accessed 20th April 2024].

Allan, P., Bryant, M., Wirsching, C., Garcia, D. & Teresa Rodriguez, M. (2013) The influence of urban morphology on the resilience of cities following an earthquake. *Journal of Urban Design*, 18(2), 242–262. Available from: https://doi.org/10.1080/13574809.2013.772881

Al-sharif, A.A.A. & Pradhan, B. (2014) Monitoring and predicting land use change in Tripoli Metropolitan City using an integrated Markov chain and cellular automata models in GIS. *Arabian Journal of Geosciences*, 7, 4291–4301. Available from: https://doi.org/10.1007/s12517-013-1119-7

Aplin, P. (2004) Remote sensing: Land cover. *Progress in Physical Geography*, 28(2), 283–293. Available from: https://doi.org/10.1191/0309133304pp413pr

14754959, 0, Downloaded from https://rgs-ibg.onlinelibrary.wiley.com/doi/10.1111/geoj.70022 by Turkey Cochrane Evidence Aid, Wiley Online Library on [19/05/2025]. See the Terms and Conditions (https://onlinelibrary.wiley.com/terms-and-conditions) on Wiley Online Library for rules of use; OA articles are governed by the applicable Creative Commons License

Aydöner, C. & Maktav, D. (2009) The role of the integration of remote sensing and GIS in land use/land cover analysis after an earthquake. *International Journal of Remote Sensing*, 30(7), 1697–1717. Available from: https://doi.org/10.1080/01431160802642289

Badri, S.A., Asgary, A., Eftekhari, A.R. & Levy, J. (2006) Post-disaster resettlement, development and change: A case study of the 1990 Manjil earthquake in Iran. *Disasters*, 30(4), 451–468. Available from: https://doi.org/10.1111/j.0361-3666.2006.00332.x

Bozkurt, E. (2001) Neotectonics of Türkiye—A synthesis. *Geodinamica Acta*, 14(1–3), 3–30. Available from: https://doi.org/10.1080/09853111.2001.11432432

Caglar, N., Vural, I., Kirtel, O., Saribiyik, A. & Sumer, Y. (2023) Structural damages observed in buildings after the January 24, 2020 Elazığ-Sivrice earthquake in Türkiye. *Case Studies in Construction Materials*, 18, e01886. Available from: https://doi.org/10.1016/j.cscm.2023.e01886

Cetin, K.O., Cakir, E., Ilgac, M., Can, G., Soylemez, B., Elsaid, A. et al. (2021) Geotechnical aspects of reconnaissance findings after 2020 January 24th, M6.8 Sivrice–Elazig–Turkey earthquake. *Bulletin of Earthquake Engineering*, 19, 3415–3459. Available from: https://doi.org/10.1007/s10518-021-01112-1

Chang, Y., Wilkinson, S., Seville, E. & Potangaroa, R. (2010) Resourcing for a resilient post-disaster reconstruction environment. *International Journal of Disaster Resilience in the Built Environment*, 1(1), 65–83. Available from: https://doi.org/10.1108/17595901011026481

Choudhary, R. & Pathak, D. (2016) Land use/land cover change detection through temporal imageries and its implications in water induced disaster in Triyuga watershed, east Nepal. *Journal of Nepal Geological Society*, 51, 49–54. Available from: https://doi.org/10.3126/jngs.v51i0.24087

Cohen, J. (1988) *Statistical power analysis for the behavioral sciences*, 2nd edition. Hillsdale, NJ: Lawrence Erlbaum Associates.

Dang, H.H. & Kawasaki, A. (2016) Review of operational land-use models. *International Journal of Agricultural and Environmental Information Systems*, 7(2), 1–25. Available from: https://doi.org/10.4018/IJAEIS.2016040101

Desalegn, T., Cruz, F., Kindu, M., Turrión, M.B. & Gonzalo, J. (2014) Land-use/land-cover (LULC) change and socioeconomic conditions of local community in the central highlands of Ethiopia. *International Journal of Sustainable Development and World Ecology*, 21(5), 406–413. Available from: https://doi.org/10.1080/13504509.2014.961181

Dewey, J.F. & Şengör, A.M.C. (1979) Aegean and surrounding regions: Complex multiplate and continuum tectonics in a convergent zone. *GSA Bulletin*, 90(1), 84–92. Available from: https://doi.org/10.1130/0016-7606(1979)90<84:AASRCM>2.0.CO;2

Dirik, K. & Göncüoğlu, M.C. (2010) Neotectonic characteristics of central Anatolia. *International Geology Review*, 38(9), 807–817. Available from: https://doi.org/10.1080/00206819709465363

Dogan, G., Ecemis, A.S., Korkmaz, S.Z., Arslan, M.H. & Korkmaz, H.H. (2021) Buildings damages after Elazığ, Turkey earthquake on January 24, 2020. *Natural Hazards*, 109(1), 161–200. Available from: https://doi.org/10.1007/s11069-021-04831-5

Duman, T.Y. & Emre, Ö. (2013) The East Anatolian Fault: Geometry, segmentation and jog characteristics. *Geological Society, London, Special Publications*, 372(1), 495–529. Available from: https://doi.org/10.1144/SP372.14

Friedl, M.A., Woodcock, C.E., Olofsson, P., Zhu, Z., Loveland, T., Stanimirova, R. et al. (2022) Medium spatial resolution mapping of global land cover and land cover change across multiple decades from Landsat. *Frontiers in Remote Sensing*, 3, 894571. Available from: https://doi.org/10.3389/frsen.2022.894571

General Directorate of Mineral Research and Exploration (MTA). (n.d.) *GeoScience map viewer and drawing editor*. Available from: http://yerbilimleri.mta.gov.tr/ [Accessed 20th April 2024].

Ghalehteimouri, K.J., Ros, F.C. & Rambat, S. (2024) Flood risk assessment through rapid urbanization LULC change with destruction of urban green infrastructures based on NASA Landsat time series data: A case of study Kuala Lumpur between 1990–2021. *Acta Ecologica Sinica*, 44(2), 289–306. Available from: https://doi.org/10.1016/j.chnaes.2023.06.007

Ghorbani Kalkhajeh, R. & Jamali, A.A. (2019) Analysis and predicting the trend of land use/cover changes using neural network and systematic points statistical analysis (SPSA). *Journal of the Indian Society of Remote Sensing*, 47(9), 1471–1485. Available from: https://doi.org/10.1007/s12524-019-00995-7

Giddings, B., Hopwood, B. & O'Brien, G. (2002) Environment, economy and society: Fitting them together into sustainable development. *Sustainable Development*, 10(4), 187–196. Available from: https://doi.org/10.1002/sd.199

Goodland, R. (2002) Sustainability: Human, social, economic and environmental. *Encyclopedia of Global Environmental Change*, 5, 481–491.

Harmanşa, A. & Abut, A. (2017) Türkiye'de kayıt dışı ekonomi gerçeği (Elazığ il örneği). *Fırat Üniversitesi Harput Araştırmaları Dergisi*, 4(1), 91–107.

Inzulza Contardo, J. & Moran Figueroa, P. (2021) Who has benefited? A socio-ecological chronology of urban resilience in the early reconstruction of Talca after the 27-F earthquake, Chile 2010–2012. *Sustainability*, 13(6), 3523. Available from: https://doi.org/10.3390/su13063523

Ishihara, M. & Tadono, T. (2017) Land cover changes induced by the great East Japan earthquake in 2011. *Scientific Reports*, 7, 44743. Available from: https://doi.org/10.1038/srep45769

Kalafat, D., Zülfikar, A.Ç. & Akçan, S.O. (2021) Seismicity of Türkiye and real-time seismology applications in determining earthquake hazard. *Academic Platform Journal of Natural Hazards and Disaster Management*, 2(2), 96–111. Available from: https://doi.org/10.52114/apjhad.1039670

Kamran, M., Khan, J.A., Khayyam, U., Waheed, A. & Khokhar, M.F. (2023) Exploring the nexus between land use land cover (LULC) changes and population growth in a planned city of Islamabad and an unplanned city of Rawalpindi, Pakistan. *Heliyon*, 9(2), e13297. Available from: https://doi.org/10.1016/j.heliyon.2023.e13297

Kandel, A., Tamir, D. & Rishe, N.D. (2014) Fuzzy logic and data mining in disaster mitigation. In: Teodorescu, H.-N., Kirschenbaum, A., Cojocaru, S. & Bruderlein, C. (Eds.) *Improving disaster resilience and mitigation-IT means and tools*. Dordrecht, the Netherlands: Springer, pp. 167–186. Available from: https://doi.org/10.1007/978-94-017-9136-6_11

14754959, 0, Downloaded from https://rgs-ibg.onlinelibrary.wiley.com/doi/10.1111/geoj.70022 by Turkey Cochrane Evidence Aid, Wiley Online Library on [19/05/2025]. See the Terms and Conditions (https://onlinelibrary.wiley.com/terms-and-conditions) on Wiley Online Library for rules of use; OA articles are governed by the applicable Creative Commons License

Kang, J., Wang, Z., Luo, X., Li, D. & Guo, X. (2022) Remote sensing land use evolution in earthquake-stricken regions of Wenchuan County, China. *Sustainability*, 14(3), 1315. Available from: https://doi.org/10.3390/su14031315

Karadeniz, E. & Sunbul, F. (2023) Land use and land cover change in Duzce region following the major earthquake: Implications for ANN and Markov chain analysis. *Environmental Earth Sciences*, 82, 243. Available from: https://doi.org/10.1007/s12665-023-10881-8

Ketin, İ. (1966) Anadolu'nun tektonik birlikleri. *Bulletin of the Mineral Research and Exploration*, 66(66), 20–37.

Khan, A.A., Arshad, S. & Mohsin, M. (2014) Population growth and its impact on urban expansion: A case study of Bahawalpur, Pakistan. *Universal Journal of Geoscience*, 2(8), 229–241. Available from: https://doi.org/10.13189/ujg.2014.020801

Krumbein, W.C. & Dacey, M.F. (1969) Markov chains and embedded Markov chains in geology. *Mathematical Geology*, 1(1), 79–96. Available from: https://doi.org/10.1007/BF02047072

Lambin, E. (2006) Land cover assessment and monitoring. In: *Encyclopedia of analytical chemistry*. Hoboken, NJ: John Wiley & Sons, Ltd.

Miller, J.P. (2020) Post-disaster recovery through the evolution of the lakou. *International Journal of Disaster Resilience in the Built Environment*, 11(1), 3–14. Available from: https://doi.org/10.1108/IJDRBE-05-2019-0021

Mondal, M.S., Sharma, N., Kappas, M. & Garg, P.K. (2020) CA Markov modeling of land use land cover change predictions and effect of numerical iterations, image interval (time steps) on prediction results. *The International Archives of the Photogrammetry, Remote Sensing and Spatial Information Sciences*, XLIII-B3-2020, 713–720. Available from: https://doi.org/10.5194/isprs-archives-XLIII-B3-2020-713-2020

Muttitanon, W. & Tripathi, N.K. (2005) Land use/land cover changes in the coastal zone of ban Don bay, Thailand using Landsat 5 TM data. *International Journal of Remote Sensing*, 26(11), 2311–2323. Available from: https://doi.org/10.1080/01431160512331326666

NASA EOSDIS. (n.d.) *ASTER global digital elevation model V003*. Earth. Available from: https://search.earthdata.nasa.gov/ [Accessed 22nd April 2024].

Natural Earth. (n.d.) *Natural Earth data*. Available from: https://www.naturalearthdata.com/ [Accessed 22nd April 2024].

Noszczyk, T. (2019) A review of approaches to land use changes modeling. *Human and Ecological Risk Assessment: An International Journal*, 25(6), 1377–1405. Available from: https://doi.org/10.1080/10807039.2018.1468994

OpenStreetMap Contributors. (n.d.) *OpenStreetMap*. Available from: https://www.openstreetmap.org/ [Accessed 22nd April 2024].

Opricovic, S. & Tzeng, G.H. (2003) Fuzzy multicriteria model for postearthquake land-use planning. *Natural Hazards Review*, 4(2), 59–64. Available from: https://doi.org/10.1061/(ASCE)1527-6988(2003)4:2(59)

Özdoğan, F., Lizarralde, G. & Herazo, B. (2024) The politics of land management after disasters: The case of post-earthquake reconstruction in Türkiye. *Disaster Prevention and Management*, 33(5), 535–560. Available from: https://doi.org/10.1108/DPM-12-2023

Pahlavani, P., Askarian Omran, H. & Bigdeli, B. (2017) A multiple land use change model based on artificial neural network, Markov chain, and multi objective land allocation. *Earth Observation and Geomatics Engineering*, 1(2), 82–99. Available from: https://doi.org/10.22059/eoge.2017.220342.1006

Petit, C., Scudder, T. & Lambin, E. (2001) Quantifying processes of land-cover change by remote sensing: Resettlement and rapid land-cover changes in south-eastern Zambia. *International Journal of Remote Sensing*, 22(17), 3435–3456. Available from: https://doi.org/10.1080/01431160010006881

Rahnama, M.R. & Wyatt, R. (2021) Projecting land use change with neural network and GIS in northern Melbourne for 2014–2050. *Australian Geographer*, 52(2), 149–170. Available from: https://doi.org/10.1080/00049182.2020.1836127

Rani, A., Gupta, S.K., Singh, S.K., Meraj, G., Kumar, P., Kanga, S. et al. (2023) Predicting future land use utilizing economic and land surface parameters with ANN and Markov chain models. *Earth*, 4(3), 728–751. Available from: https://doi.org/10.3390/earth4030039

Reilinger, R., McClusky, S., Vernant, P., Lawrence, S., Ergintav, S., Çakmak, R. et al. (2006) GPS constraints on continental deformation in the Africa–Arabia–Eurasia continental collision zone and implications for the dynamics of plate interactions. *Journal of Geophysical Research: Solid Earth*, 111(B5), B05411. Available from: https://doi.org/10.1029/2005JB004051

Renaud, F.G., Sudmeier-Rieux, K., Estrella, M. & Nehren, U. (Eds.). (2016) *Ecosystem-based disaster risk reduction and adaptation in practice*, Vol. 42. Cham, Switzerland: Springer International Publishing.

Rindfuss, R.R., Entwisle, B., Walsh, S.J., An, L., Badenoch, N., Brown, D.G. et al. (2008) Land use change: Complexity and comparisons. *Journal of Land Use Science*, 3(1), 1–10. Available from: https://doi.org/10.1080/17474230802047955

Saatcioglu, M., Mitchell, D., Tinawi, R., Gardner, N.J., Gillies, A.G., Ghobarah, A. et al. (2001) The August 17, 1999, Kocaeli (Turkey) earthquake damage to structures. *Canadian Journal of Civil Engineering*, 28(4), 715–737. Available from: https://doi.org/10.1139/l01-043

Sayın, E., Yön, B., Onat, O., Gör, M., Öncü, M.E., Tuğrul Tunç, E. et al. (2021) 24 January 2020 Sivrice-Elazığ, Turkey earthquake: Geotechnical evaluation and performance of structures. *Bulletin of Earthquake Engineering*, 19(2), 657–684. Available from: https://doi.org/10.1007/s10518-020-01018-4

Şengör, A.M.C., Tüysüz, O., İmren, C., Sakınç, M., Eyidoğan, H., Görür, N. et al. (2005) The North Anatolian Fault: A new look. *Annual Review of Earth and Planetary Sciences*, 33(1), 37–112. Available from: https://doi.org/10.1146/annurev.earth.32.101802.120415

Sharifi, A. & Yamagata, Y. (2018) Resilience-oriented urban planning. In: Yamagata, Y. & Sharifi, A. (Eds.) *Resilience-oriented urban planning: Theoretical and empirical insights*. Cham, Switzerland: Springer, pp. 3–27. Available from: https://doi.org/10.1007/978-3-319-75798-8_1

Sterling, S. & Ducharne, A. (2008) Comprehensive data set of global land cover change for land surface model applications. *Global Biogeochemical Cycles*, 22(3), 1–20. Available from: https://doi.org/10.1029/2007GB002959

Sunbul, F. (2019) An assessment of urban sprawl in northern Sakarya Province following the 1999 earthquake, NW Türkiye. *Journal of the Indian Society of Remote Sensing*, 47(9), 1487–1496. Available from: https://doi.org/10.1007/s12524-019-00988-6

Takano, T., Morita, H., Nakamura, S., Togawa, T., Kachi, N., Kato, H. et al. (2023) Evaluating the quality of life for sustainable urban development. *Cities*, 142, 104561. Available from: https://doi.org/10.1016/j.cities.2023.104561

14754959, 0, Downloaded from https://rgs-ibg.onlinelibrary.wiley.com/doi/10.1111/geoj.70022 by Turkey Cochrane Evidence Aid, Wiley Online Library on [19/05/2025]. See the Terms and Conditions (https://onlinelibrary.wiley.com/terms-and-conditions) on Wiley Online Library for rules of use; OA articles are governed by the applicable Creative Commons License

Thomas, D.S.K., Ertuğay, K. & Kemec, S. (2007) The role of geographic information systems/remote sensing in disaster management. In: Rodríguez, H., Quarantelli, E.L. & Dynes, R.R. (Eds.) *Handbook of disaster research*. Cham, Switzerland: Springer, pp. 83–95. Available from: https://doi.org/10.1007/978-0-387-32353-4_5

Tian, X., Li, W., Zhang, B., Chen, W., Chen, Z., Luo, X. et al. (2022) Spatiotemporal dynamic characteristics of land use in the typical watershed of Wenchuan earthquake-affected areas—A case study in the Longxi River basin. *Sustainability*, 14(2), 906. Available from: https://doi.org/10.3390/su142315937

Turkish Statistical Institute. (2023) *Address-based population registration system (ADNKS), results of 2023*. Available from: https://www.tuik.gov.tr [Accessed 23rd April 2024].

U.S. Geological Survey. (n.d.-a) *Earth explorer*. U.S. Department of the Interior. Available from: https://earthexplorer.usgs.gov/ [Accessed 23rd April 2024].

U.S. Geological Survey. (n.d.-b) *Earthquake catalog*. Available from: https://earthquake.usgs.gov/earthquakes/ [Accessed 23rd April 2024].

UNDRR. (2015) *Sendai framework for disaster risk reduction 2015–2030*. United Nations Office for Disaster Risk Reduction. Available from: https://www.undrr.org/publication/sendai-framework-disaster-risk-reduction-2015-2030 [Accessed 23rd April 2024].

Verburg, P.H., Schot, P.P., Dijst, M.J. & Veldkamp, A. (2004) Land use change modelling: Current practice and research priorities. *GeoJournal*, 61(4), 309–324. Available from: https://doi.org/10.1007/s10708-004-4946-y

Wang, J., Su, Y., Wang, H., Zhang, Y. & Ma, L. (2022) Land cover changing pattern in pre- and post-earthquake affected area from remote sensing data: A case of Lushan County, Sichuan Province. *Landscape*, 11(1), 117. Available from: https://doi.org/10.3390/land11081205

Weng, Q. (2001) Modeling urban growth effects on surface runoff with the integration of remote sensing and GIS. *Environmental Management*, 28(6), 737–748. Available from: https://doi.org/10.1007/s002670010258

Wu, J. & Wu, T. (2012) Ecological resilience as a foundation for urban design and sustainability. In: Pickett, S.T.A., Cadenasso, M.L. & McGrath, B. (Eds.) *Resilience in ecology and urban design: Linking theory and practice for sustainable cities*. Dordrecht, the Netherlands: Springer, pp. 211–229. Available from: https://doi.org/10.1007/978-94-007-5341-9_10

How to cite this article: Sunbul, F., Karadeniz, E., Sengun, M.T. & Kocaoglu, M. (2025) Forecasting urban shifts post-earthquake: LULC change analysis in Elazığ, Turkey using ANN and Markov models. *The Geographical Journal*, 00, e70022. Available from: https://doi.org/10.1111/geoj.70022

14754959, 0, Downloaded from https://rgs-ibg.onlinelibrary.wiley.com/doi/10.1111/geoj.70022 by Turkey Cochrane Evidence Aid, Wiley Online Library on [19/05/2025]. See the Terms and Conditions (https://onlinelibrary.wiley.com/terms-and-conditions) on Wiley Online Library for rules of use; OA articles are governed by the applicable Creative Commons License